23nd IAHR International Symposium on Ice

Ann Arbor, Michigan USA, May 31 to June 3, 2016

The tensile strength of saline and freshwater ice in field tests

P. Chistyakov[1,3], E. Karulin[4,3], A. Marchenko[2,3], A. Sakharov[1,3], B. Lishman[3,5]
[1] Moscow State University, Moscow, RUSSIA
[2]The University Centre in Svalbard, Longyearbyen, NORWAY
[3]Sustainable Arctic Marine and Coastal Technology (SAMCoT), Centre for Research-based Innovation (CRI), Norwegian University of Science and Technology, Trondheim, NORWAY
[4] Krylov State Research Centre, St.-Petersburg, RUSSIA
[5]Portsmouth University, Department of Engineering, UK
[*]chist206@yandex.ru

This paper presents the results of meso-scale (~1m) in-situ tests on the tensile strength of saline and freshwater floating ice. These results are directly comparable to previous small scale tests, in which the measured tensile strength of sea ice and fresh ice decreases from 1MPa to 0.2MPa as the temperature increases from -30C to -2C. The new experiments were performed in Svalbard, Norway, from 2013-16, on landfast ice in the Van Mijen Fjord, and on freshwater lake ice near Longyearbyen. Loads were applied in the horizontal direction over the entire ice thickness on pre-cut necks, described below. All meso-scale tests demonstrated brittle and synchronous failure of the necks by tension. Values of meso-scale tensile strength are typically around 0.1MPa.

1. Introduction

The tensile strength of sea ice is much smaller than the compressive strength. Despite this, the tensile strength is important when the ice fails in bending. Simple models of bending strength assume that the ice fails when stresses on the surface (top or bottom) of the ice reach the tensile strength. The tensile strength also represents an important reference point for describing the principal stresses when formulating failure criteria for ice (see e.g. Timco and Frederking, 1986; Iliescu and Schulson, 2004). The minimum tensile strength of sea ice measured in laboratory experiments is about 0.2MPa, which is several times lower than the lowest measurements of of compressive strength, around 1MPa (Timco and Weeks, 2010). In large-scale models of sea ice dynamics, ice is characterised by a constant compressive strength of p*~5kPa, and assumed to have zero resistance to tensile deformations (see e.g. Pritchard, 2001). Any scale effects in measurements of tensile strength may be important in understanding meso-scale problems related to e.g. the stability of landfast ice, the marginal ice zone, etc.

Tests on tensile strength are usually performed with cylindrical cores taken (horizontally or vertically) from floating ice or from ice grown in the laboratory. One complication in such tests is the question of how to fix the ends of the cores. Usually the core ends are fixed in similar coaxial caps with ears, and a tensile load applied to the caps. Details of experiments on tensile strength are descibed in several papers (e.g. Dykins, 1970; Kuehn et al., 1990; Richter-Menge and Jones, 1993; Sammonds et al., 1998). All of these papers describe laboratory experiments.

The flexural strength of ice can be measured directly and used to formulate bending failure criteria. Flexural strength tests are performed with ice beams sawn and removed from the ice, and with floating cantilever beams (see e.g. Lainey and Tinawi, 1981; Timco and Weeks, 2010). In flexural strength tests beams are broken by direct bending, but the effects of stress concentrations near beam edges and roots may influence the results. Similarly, stress concentrations may occur near the ends caps in small-scale tensile strength tests. Other complications in small-scale tensile strength tests include the possibility that ice cores, once removed, exhibit different material properties to natural ice, and the difficulty of performing tests on warm saline ice close to its melting point.

In the present paper we describe original meso-scale tensile strength tests performed in-situ. The test results are compared with the results of standard small-scale tensile strength tests, performed on ice from the same location, and with the results of in-situ flexural strength tests on cantilever floating beams.

2. Experimental procedure

In-situ experiments on the tensile strength of floating ice were performed in three different configurations. Schematics of the experiments I, II and III are shown in Fig.1a, Fig.1b and Fig.1c respectively. In tests I and II the tensile force is supported across two necks. In test 1 the necks are elongated in the loading direction. Preparation of this test requires accurate and time-consuming layout and sawing. In test II the necks are located between drilled holes of radius R=35cm. Preparation of this test is less time-consuming than test I. Photographs of tests I and II are shown in Fig.2a and Fig.3a respectively.

The load is applied by the bespoke rig shown in Fig.4a, in which two hydraulic cylinders connect two steel loading plates. The rig was designed and constructed in a collaboration between UNIS (Svalbard, Norway), MK Lund Ltd., (Oslo, Norway) and Krylov State Research Center (St.-Petersburg, Russia). In some experiments vertical steel half-cylinders were used instead of the flat steel plates. The hydraulic cylinders (Enerpac, 30T) are controlled by an eletrical station powered by a three-phase generator and steered by a bespoke field computer. Loads are measured with loads cells installed inside the hydraulic cylinders, and with a load cell (HBM 10T) placed in front of the indenting steel plate, fixed on a wooden beam (Fig.2b). This second load cell is used specifically to measure the relatively small loads required in tension tests.

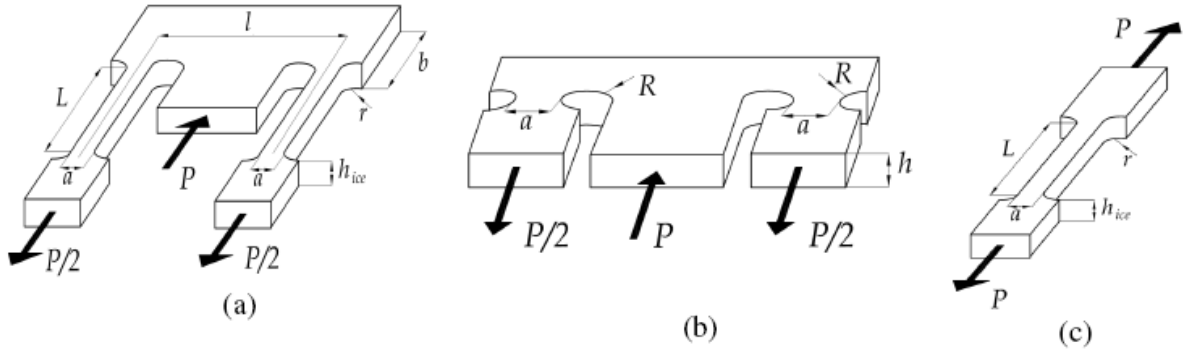

Figure 1. Experimental schematics of tensile strength tests I(a), II(b) and III(c) performed on floating ice.

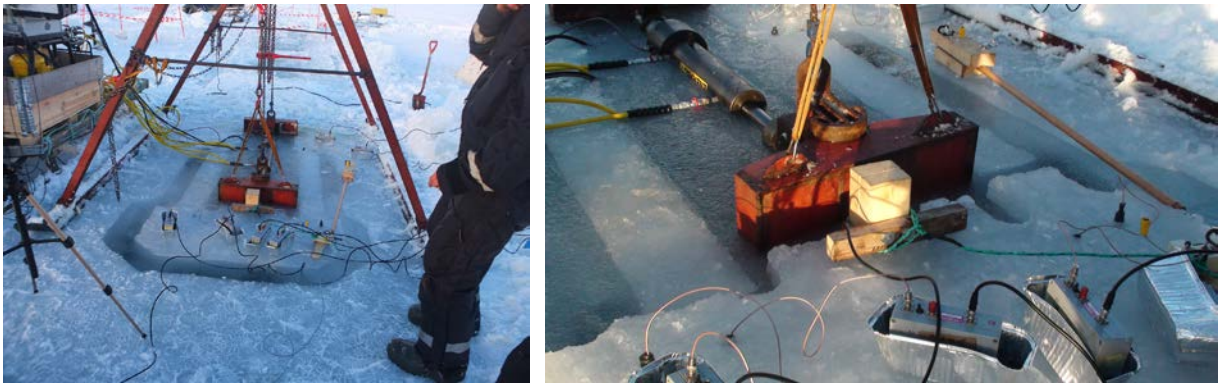

a) b)

Figure 2. Photographs of test I before (a) and after (b) the test.

a) b)

Figure 3. Photographs of test II before (a) and after (b) the test.

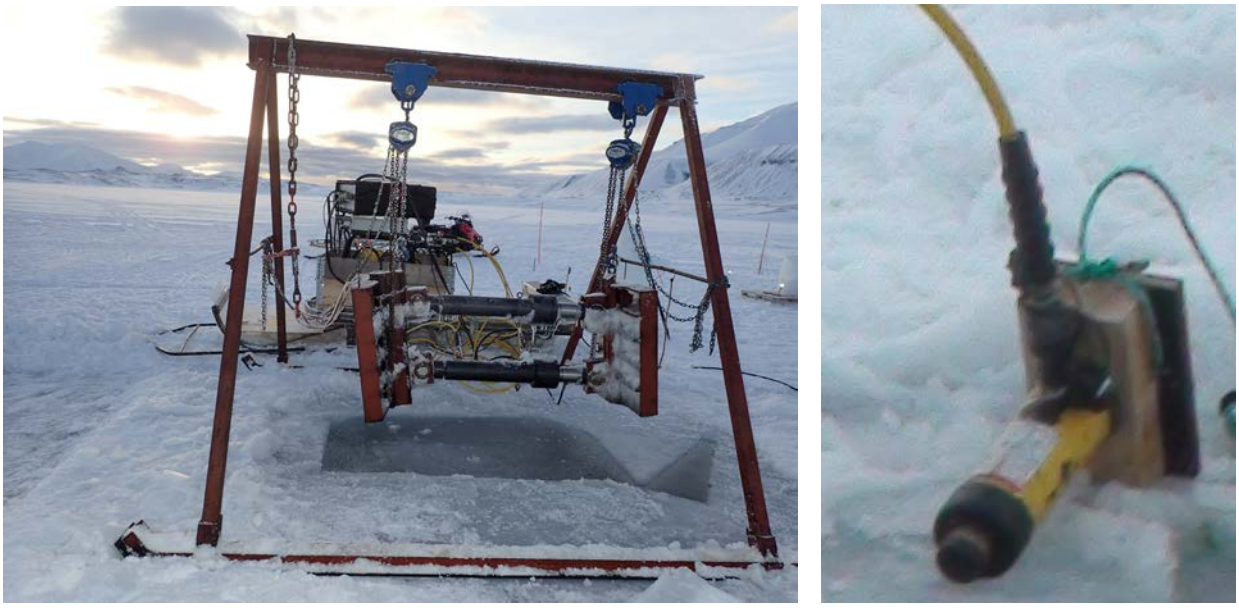

a) b)

Figure 4. Indentation rig with two hydraulic cylinders (a). Hydraulic cylinder used in test III and in small scale tensile strength tests (b).

Displacements are measured with stroke sensors installed inside the hydraulic cylinders, and with original displacement sensors designed in the Institute of Mechanics of MSU (Moscow, Russia) for the tests. Each of the two sensors is mounted on an ice neck, and extends in tension along with the neck. When tensile deformation of the neck occurs, the wooden beam shown in Fig.5b pulls the displacement transducer shown in Fig.5a. The displacement transducers can thus measure the failure time of the necks (since failure leads to a large displacement) and can give an indication of whether failure occurred simultaneously in both necks in tests I and II.

a) b)

Figure 5. Displacement sensor for the measurement of the neck deformations.

In test configuration III, there is only one neck, and the ice fails on this neck during the test. The test configuration is shown in figure 6. An ice neck and head are sawn in floating ice. A vertical hole (10cm diameter; drilling hole 1 in Fig.6c) is drilled in the ice head. A second hole is drilled behind the ice neck (drilling hole 2 in Fig.6c). A plastic torus was placed in each hole, and in each torus a steel splint (M24) was screwed. Wooden beams, above and below the ice, joined these two splints (the beam above the ice can be seen in figure 6a). Loads were applied

horizontally on wooden beams 1 and 2 by a 15T Enerpac hydraulic cylinder, via a 10T HBM load cell sandwiched between two wooden plates. The displacement sensor described above was used to measure deformation of the neck, and is visible on the right hand side of Fig.6a and Fig.6b.

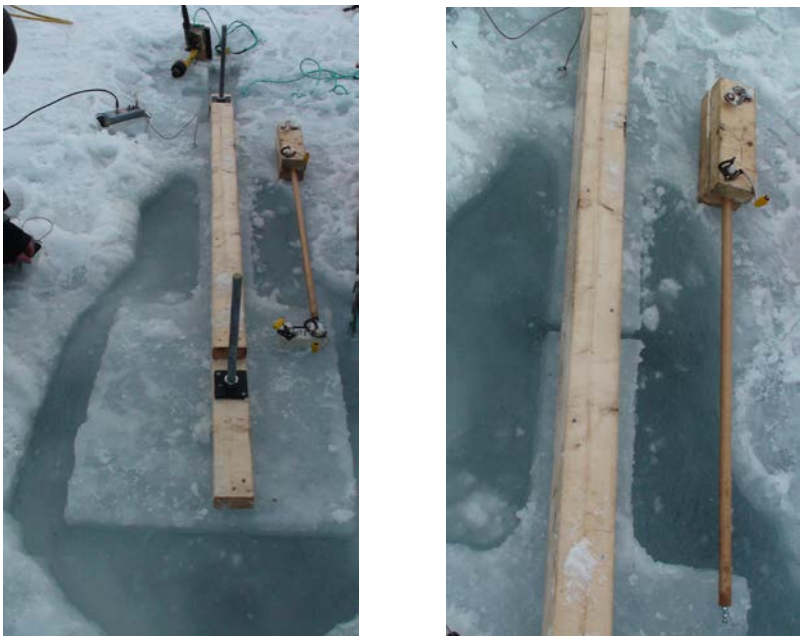

a) b)

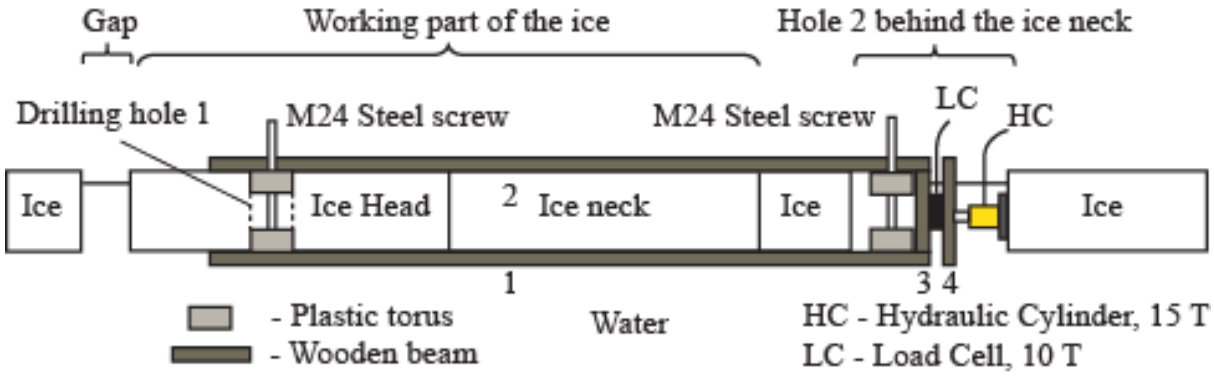

c)

Figure 6. Photographs of test III before (a) and after (b) the ice failure. Instrumentation scheme for test III (c).

Small-scale tensile strength tests were performed in March 2016 using a bespoke rig designed at UNIS. Horizontal ice core samples of 72.5mm diameter were drilled (with a Kovacs ice drill) from the blocks removed from the sea ice during preparation of the tests above. The ends of these cores were frozen, with distilled water, into cylindrical steel caps with a grooved inner surface. Steel rods mounted on the cap surface were used to ensure they remained coaxial during

the freezing process. The freezing time was several hours. During this time the ice sample temperature tends towards the air temperature.

The ice sample, frozen between the end caps, was placed into the rig and fixed in place between a load cell and the rig bottom (Fig.7). Loads are applied by a hydraulic cylinder (Enerpac 15T) mounted on the steel frame. Axial deformations are measured with an EpsilonTech extensometer, with 50mm base, mounted in the middle part of the ice sample (Fig.7b). The apparatus was powered by an electrical pump and three-phase generator.

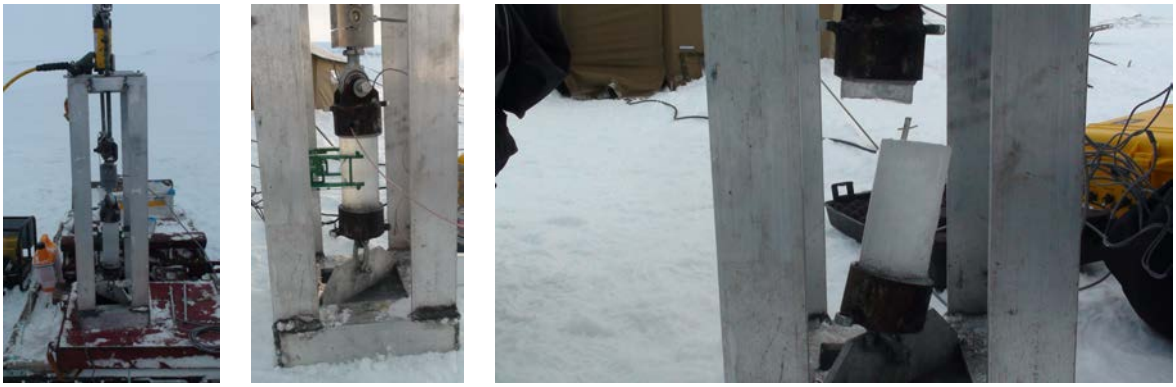

a) b) c)

Figure 7. Rig for small scale tensile strength tests (a). Ice sample in the rig before the test (b). Ice sample after the test (c).

During tests in 2016, acoustic emissions (AE) were measured for one meso-scale test in configuration I, one meso-scale test in configuration III, and three small-scale tests. AE were measured using a Vallen Amsy-5 Acoustic Emission System, with bespoke transducers designed at University College London, based on 15mm compressional piezo crystals with a cutoff frequency of 500kHz. Acoustic emissions are generated when ice deforms: crack growth, friction and yielding produce mechanical waves in the ice which are detected by the apparatus. Sound waves between 100Khz and 500kHz generate electric pulses in the piezo transducers, which are amplified locally. If these pulses exceed a certain threshold, the apparatus registers a 'hit', a discrete event with a known time and amplitude. The results from AE measurements can complement the load/displacement data, giving a sense of where and when the ice was deforming.

Data from all tests - loads and deformations as a function of time - are measured on a Campbell 1000 data logger with sampling frequency 100Hz.

3. Test results

Meso-scale tensile strength tests in Svalbard have performed since October-November 2013 on fresh water in a small lake near Mine 7 in Longyearbyen; in March 2014 and March 2015 on sea ice in Svea near the coal quay at Kapp Amsterdam; and in March 2016 in the Vallunden lake, which is connected by a narrow strait to the Van Mijen Fjord in the vicinity of Svea. The salinity of the sea water in the fjord and in the Vallunder lake are similar (~34-35 PSU) and the ice salinity is also similar (4-7ppt). THe conditions of ice formation in the Vallunden lake are different from the sea, because of less slush and strongly damped waves. Two meso-scale tensile

strength tests performed on the fresh water lake in 2013 and 2014 were unsuccessful because the data were not stored on the field computer. Later the data logger was installed to provide parallel and independent data storage.

Table 1. Characteristics of meso-scale tensile strength tests

	Date	Type	Location	h_i, mm	L, mm	a, mm
1	2013-11-01	II	Mine 7	410	-	150
2	2014-03-29	I	KA	450	1000	250
3	2014-10-30	II	Mine 7	500	-	150
4	2015-03-17	II	KA	730	-	160
5	2015-11-04	I	Mine 7	420	800	150
6	2016-03-07	III	Vallunden	570	800	200
7	2016-03-09	I	Vallunden	570	1000	200

The geometry of the meso-scale tests, which varies between tests I, II and III (Fig.1), is important. Test I, with long necks, looks the most standard, but may be unstable due to the difficulty of cutting straight necks. Ice preparation is particularly complicated when the ice surface is covered by a thick layer of snow mixed with water. Preparation of test II is simpler, but the working length of the narrowing between drilled holes is very short, and so the deformation may not be pure tension. In all tests the ice failed on the necks and near the narrowings (e.g. Fig.2b, Fig.3b).

Table 2. Results of meso-scale tensile strength tests

	Data	Type	σ_{max}, MPa	E, MPa	T_a, C	S_i, ppt
2	2014-03-29	I	0.098	-	-10	6
4	2015-03-17	II	0.087	-	-11	5
5	2015-11-04	I	0.197	3070	-11	0
6	2016-03-07	III	0.147	-	-5	4
7	2016-03-09	I	0.151	1250	-5	4

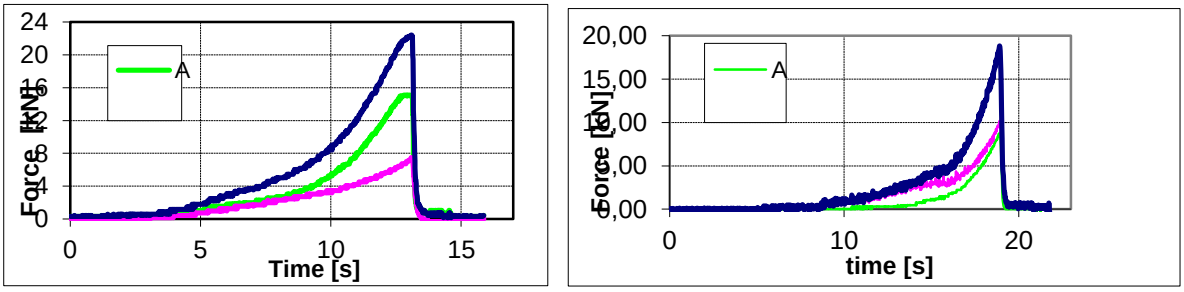

a) b)

Figure 8. Loads in hydraulic cylinders versus time measured in the tests 2 (a) and 4 (b).

All meso-scale tests demonstrate brittle failure of ice in tension (Fig.8, Fig.9a, Fig.10). The strain rate in test 5, estimated from Fig.7b, is about $3 \cdot 10^{-6} s^{-1}$. Meso-scale tensile strength of sea ice near Kapp Amsterdam is somewhat smaller than 0.1 MPa, and meso-scale tensile strength of sea ice in the Vallunden Lake is around 0.15 MPa. The difference is explained by the ice structure. The ice near Kapp Amsterdam was very inhomogeneous and some ice layers were probably

formed from slush. The ice in the Vallunden Lake is more homogeneous and solid. It is interesting that tests 6 (Type I) and 7 (Type II) shown very close values of the tensile strength. Test 5, performed on fresh water ice, gave the highest tensile strength: close to 0.2 MPa.

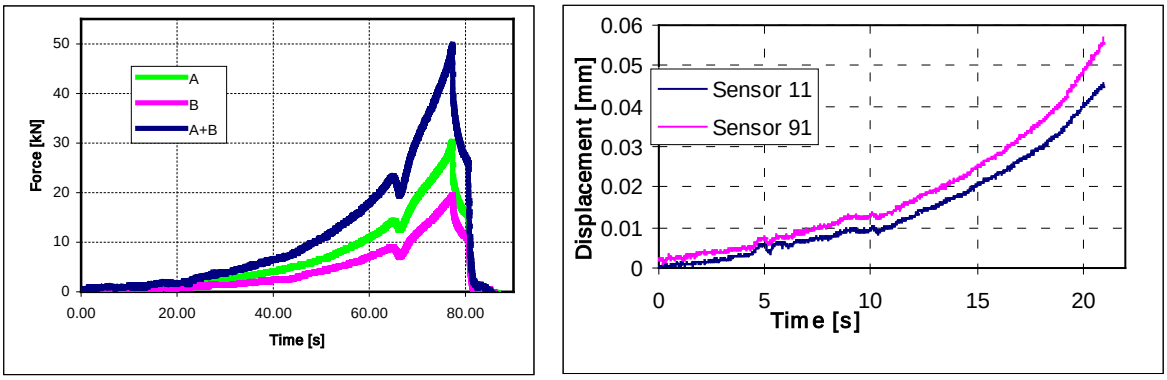

a) b)

Figure 9. Loads in hydraulic cylinders (a) and displacements in the necks (b) measured in test 5.

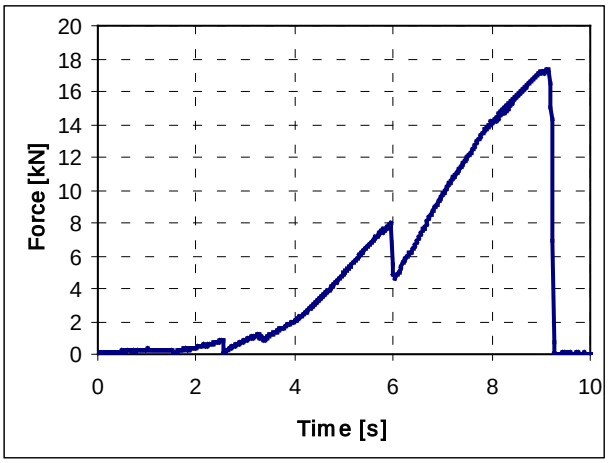

Figure 10. Load versus time in test 6 (Table 2).

Small-scale tests demonstrated relatively high tensile strength, varying from 0.4 to 0.63 MPa. Their salinity and temperature were lower than in sea ice because the samples were hanging for several hours in the air. These values correspond to tensile strength values measured in previous experiments (Timco and Weeks, 2010). Values of the effective elastic modulus calculated from meso-scale tests are smaller than the elastic modulus calculated from small scale tests. For example the elastic modulus is 1.25 GPa in test 7, and 3.6 GPa in small scale test 4.

Table 3. Results of small-scale tensile strength tests

	Data	S_i, ppt	T_a, C	L, m	$\sigma_{max,}$ MPa	E, GPa
1	2016-03-06	1.68	-5.4	0.188	0.418	-
2	2016-03-06	1.14	-5.1	0.135	0.598	-
3	2016-03-08	2.20	-6.0	0.250	0.630	-
4	2016-03-08	2.20	-6.5	0.230	0.439	3.6 GPa

Preliminary analysis of the acoustic emissions suggests that the amplitude of emissions are well correlated with the force during tensile tests. Further, the arrival times of individual events can be used to determine the approximate location of those events, and to understand the precise timings of near-synchronous events like the failure of the two arms in test 7. These results (which will be presented in full elsewhere) suggest that AE recording can be a useful add-on to meso-scale field tests like those in this paper.

4. Discussion

2D finite element modeling was performed to investigate deformations of the ice necks during the tests. The stress distribution in the sample depends strongly on the bending rigidity of the cross-beam connecting the necks. The bending moment M which occurs in the beam shoulders (Fig.13b) can be evaluated by dimensionless value $e=2M/(aP)$, where P is the applied load. Relative eccentricity e and stress concentration σ_{max}/σ_0 were calculated for different ratios l/a and b/a of the cross-beam. The fillet radius r in each simulation equals $a/2$. Analyzing data from numerical simulations we see that the influence of the reactive bending moment is small for a cross-beam with large height. When the rigidity of the cross-beam increases ($b/a>5$) the stress concentration in the root is determined by the fillet radius only. In any case the tensile stress reaches its maximum near the inner fillet of the root. The ice failure in test 7 was observed in precisely this place.

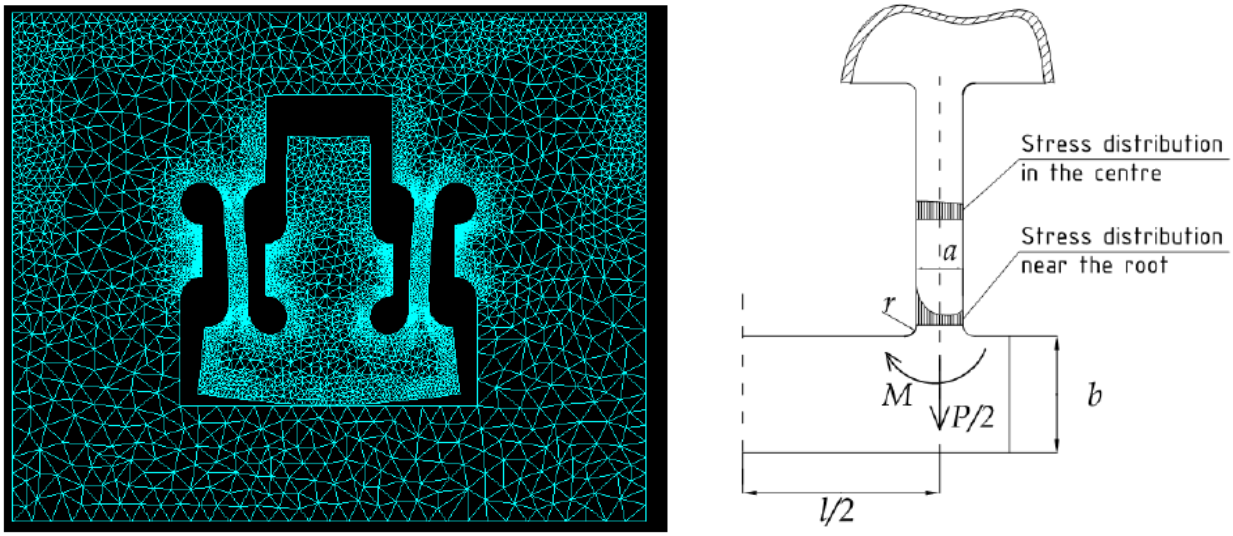

a) b)

Figure 13. Computational domain and zoomed deformations in test I (a). Stress distribution in two cross-section of the ice neck (b).

In spite of the calculated stress concentration near the fillet the tensile strength was similar in tests 6 with a single neck and test 7 with two necks. Stress concentrations near the root fillets have also been discovered in the tests with cantilever beams (see, e.g., Frederking and Svec, 1985; Marchenko et al., 2014). Nevertheless tests performed with different fillet radiuses show similar values of the flexural strength. The physical mechanism of the stress concentration damping may relate to plastic deformations and should be further investigated.

5. Conclusions

Original in-situ meso-scale tests were performed on fresh and sea ice to measure tensile strength. Measured values of the tensile strength vary from 0.1 to 0.15 MPa in sea ice. This is 1.5-2 times lower than the minimal values of tensile strength registered in earlier small scale experiments. The difference can be explained by temperature gradient through the ice, and the high temperature of the bottom ice layer in the meso-scale tests. The meso-scale tensile strength of 0.15 MPa was lower than the flexural-strength of 0.2 MPa measured in tests (in March 2016) with floating cantilever ice beams loaded upward.

Acknowledgments

The authors wish to acknowledge the support of the Research Council of Norway through the Center for Sustainable Arctic Marine and Coastal Technology (SAMCoT)

References

Dykins, J E. 1970. Ice engineering: tensile properties of sea ice grown in a confined system. Port Hueneme, CA, Naval Civil Engineering Laboratory. (NCEL Technical Report R680)

Frederking, R.M.W., Svec, O.J. , 1985. Stress-relieving techniques for cantilever beam tests in an ice cover. *Cold Reg. Sci. Tech.*, 11:247-253.

Iliescu, D., Schulson, E.M., 2004. The brittle compressive failure of fresh-water columnar ice loaded bi-axially. *Acta Materialia*, 52 (20), 5:723–5,735.

Kuehn, G. A., R. W. Lee, W. A. Nixon and E. M. Schulson. 1990. The structure and tensile behavior of first-year sea ice and laboratory grown saline ice. *ASME Journal of Offshore Mechanics and Arctic Engineering*, 112(4): 357-363.

Lainey, L., Tinawi, R., 1981. The mechanical properties of sea ice — a compilation of available data. *Canadian Journal of Civil Engineering*, 11 (4): 884–923.

Marchenko, A., Karulin, E., Chistyakov, P., Sodhi, S., Karulina, M., Sakharov, A., 2014. Three dimensional fracture effects in tests with cantilever and fixed ends beams. *22th IAHR Symposium on Ice*, Singapore, paper 1178.

Pritchard, R.S., 2001. Sea ice dynamics models. J.P.Dempsey and H.H.Shen (eds.), *IUTAM Symposium on Scaling Laws in Ice Mechanics and Ice Dynamics*, Kluwer Academic Publishers, Dordrecht: 265-288.

Richter-Menge, J.A., Jones, K.F., 1993. The tensile strength of first year sea ice. *J. Glaciology*, 39(133): 609-618.

Sammonds, P.R., Murrell, S.A.F., Rist, M.A., 1998. Fracture of multiyear sea ice. *J.Geoph. Res*., 103(NC10): 21,795-21,815.

Timco, G.W., Frederking, R.M.W., 1984. An investigation of the failure envelope of granular/discontinuous-columnar sea ice. *Cold. Reg. Sci. Techn*., 9: 17–27.

Timco, G.W., Weeks, W.F., 2010. A review of the engineering properties of sea ice. *Cold. Reg. Sci. Techn*., 60: 107-129.